When the woolly rhinoceroses roamed East Asia: a review of isotopic paleoecology of the genus *Coelodonta* from the Tibetan Plateau to northern Eurasia

Jiao Ma[1,2], Shiqi Wang[1] and Tao Deng[1,3]*

[1]Key Laboratory of Vertebrate Evolution and Human Origins of Chinese Academy of Sciences,
Institute of Vertebrate Palaeontology and Palaeoanthropology, Chinese Academy of Sciences,
Beijing, China, [2]State Key Laboratory of Palaeobiology and Stratigraphy, Nanjing Institute of Geology
and Palaeontology, Chinese Academy of Sciences, Nanjing, China, [3]University of Chinese Academy of
Sciences, Beijing, China

East Asia, being the evolutionary center of *Coelodonta*, offers a unique opportunity to explore the spatiotemporal paleoecologies of this genus. This study utilized bulk and serial stable carbon and oxygen isotope analyses on the *Coelodonta nihowanensis* and other ungulates from the Longdan fauna as well as two modern goats in the Linxia Basin, aiming to explore the paleoecology of *C. nihowanensis* at the periphery of the Tibetan Plateau during the Early Pleistocene. The isotopic results of these mammals indicated that C_3 vegetation was possibly a major component of the local environment in the Linxia Basin, which was influenced by a seasonal summer monsoon. *C. nihowanensis* specimens in the Longdan fauna were possibly mixed feeders, as indicated by the wide distribution of their $\delta^{13}C$ values and the intermediate $\delta^{18}O$ values compared to other coexisting ungulates. Moreover, the comparison of the $\delta^{13}C$ and $\delta^{18}O$ values of similar taxa from the Linxia and Nihewan basins has revealed spatiotemporal differences in the paleoclimate and paleoenvironments of these two regions throughout the Early Pleistocene. This provides a holistic framework for understanding the paleoecology of the *C. nihowanensis*. The isotopic results of the *C. nihowanensis* in the Linxia and Nihewan basins suggested varied foraging ecologies across different sites and time spans during the Early Pleistocene. This underscores the adaptability of the *C. nihowanensis* to diverse environments from west to east in northern China. By scrutinizing the evolutionary ecological history of the woolly rhinoceroses from its ancestor, *Coelodonta thibetana*, to its final form, *Coelodonta antiquitatis*, this study sheds light on the ecological adaptation of this genus from the Pliocene to Late Pleistocene, spanning its migration from the Tibetan Plateau to northern Eurasia.

1 Introduction

As the final representative of the woolly rhinoceroses, *Coelodonta antiquitatis* stands as an iconic species thriving on the mammoth steppe during the Late Pleistocene, with its distribution extending widely across northern Eurasia (Kahlke and Lacombat, 2008; Kahlke, 2014). However, East Asia has long been considered the cradle and evolutional center of the genus *Coelodonta*.

Deng et al. (2011) documented the earliest known ancestor of the woolly rhinoceroses, *Coelodonta thibetana*, originating from the Zanda Basin in the southwestern Tibetan Plateau at 5.08 Ma (Deng et al., 2011; Wang X. et al., 2013). This species then evolved into *Coelodonta nihowanensis*, which mainly thrived in northern China during the Early Pleistocene (Deng, 2002, 2008; Jin et al., 2021). *C. nihowanensis* in the Linxia Basin was considered to be the earliest woolly rhinoceros (2.5–2.2 Ma) prior to the discovery of the *C. thibetana* (Qiu et al., 2004; Deng, 2006; Zan et al., 2016; Deng et al., 2023). *C. nihowanensis* then dispersed out the Tibetan region, and it was commonly found in multiple sites in northern China, including the Nihewan Basin and Jinyuan Cave during the Early Pleistocene (e.g. Tong and Wang, 2014; Chen et al., 2017; Dong et al., 2021; Chen et al., 2023). *C. nihowanensis* gradually evolved into *Coelodonta tologoijensis* and was discovered in Russia and Mongolia during the early Middle Pleistocene. Its occurrence in Europe is still in debate (Kahlke and Lacombat, 2008; Uzunidis et al., 2022). *Coelodonta* then terminated in *C. antiquitatis* and its distribution extended over approximately 190° of longitude and 40° of latitude (Kahlke, 1999; Stefaniak et al., 2023). Through the evolutionary history of the woolly rhinoceroses, the genus *Coelodonta* was restricted in East Asia for more than 4 million years. Therefore, delving into the paleoecological shifts within *Coelodonta* in East Asia becomes essential for a deeper comprehension of the interplay between its evolutionary dynamics and the paleoenvironmental changes.

The series of morphological traits of *Coelodonta*, including special nasal horn, a low position of the head, and complex tooth morphology, were all considered indicators of grazing in cold and dry environment (Fortelius, 1983; Kahlke and Lacombat, 2008; Deng et al., 2011). As the most emblematic member of *Coelodonta*, the paleoecology of *C. antiquitatis* was intensively explored through various methods, and it was evidenced as a cold-adapted grazer (e.g. Rivals et al., 2010; Pushkina et al., 2020). The stable isotope analysis was applied on *C. thibetana* and *C. nihowanensis* in the Zanda and Nihewan basins. *C. thibetana* in the Zanda Basin fed on C_3 vegetation in an environment dominated by C_3 plants (Wang Y. et al., 2013), and *C. nihowanensis* in the Nihewan Basin displayed different foraging ecologies at different sites (Xu et al., 2021; Xu et al., 2023). The presence of *C. nihowanensis* in the Linxia Basin suggests a connection between the mid-Pliocene Zanda Basin and the Early Pleistocene Nihewan Basin (Deng et al., 2023). This provides an opportunity to explore the paleoecological changes of *Coelodonta* as they migrated out of the Tibetan Plateau. The previous study explored the paleoecology of Cenozoic rhinoceroses in the Linxia Basin; however, only one *C. nihowanensis* specimen was analyzed and identified as a grazer in the Longdan fauna (Biasatti et al., 2018). It is evident that more specimens are required to investigate the dietary ecology of *C. nihowanensis* in the Linxia Basin. Furthermore, all isotopic data from East Asia should be discussed from the perspective of the *Coelodonta* evolution.

In this study, we performed stable carbon and oxygen isotope analyses on *C. nihowanensis* and other ungulates from the Longdan fauna to investigate the paleoecology of *C. nihowanensis* in the Linxia Basin during the Early Pleistocene. Additionally, we conducted an extensive review of all published isotopic data pertaining to *Coelodonta* and coexisting mammals, aiming to provide a deeper understanding of the paleoecological shifts experienced by *Coelodonta* in East Asia.

2 Carbon and oxygen isotopes in tooth enamel

Higher plants are generally divided into C_3 (including virtually all trees, most shrubs and herbs, and cool-season grasses), C_4 (warm season grasses), and CAM (succulents) plants according to different photosynthesis pathways (Troughton and Card, 1975; O'Leary, 1981; Farquhar et al., 1989). Modern C_3 plants have an average $\delta^{13}C$ value of −25‰, while C_4 plants have an average $\delta^{13}C$ value of −13‰ (Bender, 1968; Smith and Epsten, 1971; Kohn and Cerling, 2002). Additionally, water use efficiency, the canopy effect, natural physiology, and abiotic factors can impact the $\delta^{13}C$ values of plant tissues (van der Merwe and Medina, 1991; Quade et al., 1995; Peuke et al., 2006; Kohn, 2010). When plants are directly consumed by mammals, isotopic fractionation occurs during the process of tissue formation. The enrichment factors between plant consumption and tooth enamel bioapatite are roughly 14‰ for herbivores, although they may be slightly influenced by variations in their body sizes and digestive strategies (Ambrose and Norr, 1993; Cerling and Harris, 1999; Kohn and Cerling, 2002; Tejada-Lara et al., 2018; Cerling et al., 2021). A tooth enamel with a $\delta^{13}C$ value of less than −9‰ generally indicates a pure C_3 diet, while a $\delta^{13}C$ value greater than −2‰ would demonstrate a pure C_4 diet (Cerling et al., 1997). Nevertheless, in water-stressed environments, a conservative enamel-$\delta^{13}C$ value cut-off for a pure C_3 diet in fossil herbivores should likely be −7‰ or even −6.5‰ (Cerling et al., 1997; Wang et al., 2008a). Therefore, the $\delta^{13}C$ values of mammals are valuable for reconstructing their paleodiet and paleoecology. Nonetheless, recent researches have uncovered that the relationships between herbivore assemblages and the vegetation landscapes are complicated (Negash and Barr, 2023; Sokolowski et al., 2023), underscoring the importance to avoid simplistic interpretations of paleolandscapes based solely on the $\delta^{13}C$ values of fossil herbivores.

The $\delta^{18}O$ values in the bioapatite of the mammal bones and teeth are primarily determined by the source of water consumed and their foraging ecology (Bryant and Froelich, 1995; Pederzani and Britton, 2019). For large herbivores relying heavily on drinking water, the $\delta^{18}O$ values derived from tooth enamel directly reflect the $\delta^{18}O$ values they consume, which can vary due to factors, such as local temperature, precipitation, and humidity (Dutton et al., 2005; Pederzani and Britton, 2019). In general, tree leaves exhibit higher $\delta^{18}O$ values than grasses due to increased transpiration of water (Koch et al., 1989; Quade et al., 1995). Consequently, herbivores

relying on such foliage typically demonstrate higher δ^{18}O values than those consuming grasses.

Mammalian teeth form incrementally from the top to the bottom of the tooth crown during the period of tooth growth (Hillson, 2005). Once tooth enamel is fully mineralized, it remains unaltered throughout the lifespan of mammals, thereby preserving the isotopic sequence formed during its development (Suga, 1979). Consequently, bulk sampling of the entire height of tooth enamel can be used to reconstruct the average diet and ecology during the tooth formation period, while serial sampling of the tooth enamel along the direction of enamel growth can offer detailed insights into the dietary and ecological changes of mammals (Kohn et al., 1998; Balasse, 2002; Blumenthal et al., 2014, Blumenthal et al., 2019; Li et al., 2020). However, enamel mineralization progresses in a non-linear manner, following distinctive trajectories within the enamel layers that do not consistently align with incremental growth lines (Suga, 1979; Smith et al., 2003). Therefore, conventional serial sampling method often yields composite samples from multiple enamel layers, which may potentially dampen seasonal signals (Sharp and Cerling, 1998; Higgins and MacFadden, 2004; Green et al., 2018).

3 Materials and methods

3.1 Geological settings and sample selection

The Linxia Basin, located on the northeastern edge of the Tibetan Plateau, is well known for its thick and continuous Late Cenozoic deposits and its exceptionally rich and diverse mammalian fossils (Deng et al., 2013). The Longdan, the first Early Pleistocene site in China discovered from loess, belongs to the Wucheng Formation, characterized by yellowish hard loess with layers of calcite concretions (Qiu et al., 2002; Qiu et al., 2004). Magnetostratigraphic dating had determined the age of the Longdan fauna to be 2.5–2.2 Ma (Zan et al., 2016). This fauna has yielded abundant fossils of 33 mammalian species, including *Equus eisenmannae*, *Proboscidipparion sinense*, *C. nihowanensis*, *Leptobos brevicornis*, and a diverse range of carnivores (Qiu et al., 2004). The mammalian fossils in the Longdan fauna exhibit slightly more primitive features than those of the Early Pleistocene Nihewan fauna (Qiu et al., 2004). The Nihewan fauna represents another significant Early Pleistocene mammalian assemblage in northern China, preserving abundant *C. nihowanensis* fossils, and its geological age are 2.4–1.8 Ma or 2.2–1.7 Ma (Qiu, 2000; Liu et al., 2012; Farjand et al., 2023a; Farjand et al., 2023b). *E. eisenmannae* in the Longdan fauna was one of the earliest and most primitive *Equus* in Eurasia, while *C. nihowanensis* in this fauna was initially regarded as the most primitive woolly rhinoceros before the discovery of the *C. thibetana* (Qiu et al., 2004; Deng, 2006).

3.2 Materials

27 fossil tooth samples were collected from the Longdan fauna, including the woolly rhinoceros *C. nihowanensis* (n=7), the deer

Nipponicervus longdanensis (n=4), Bovinae (*L. brevicornis* and *Hemibos gracilis*) (n=7), and the gazelle *Gazella* cf. *blacki* (n=9). These specimens were housed in the Institute of Vertebrate Paleontology and Paleoanthropology and the Hezheng Paleozoological Museum in China. However, the precise stratigraphic levels of these tooth specimens were not recorded. Two modern goats were collected as modern references. Among them, 8 fossil samples and 2 modern goats were serially sampled. In total, 103 specimens were collected.

3.3 Stable isotope analysis

First, the teeth were cleaned by removing a very thin (~0.1 mm) layer of outer enamel using a diamond-tipped dental burr. For bulk samples, enamel powder was collected from the entire range of tooth heights to obtain an average value. Well-preserved teeth with complete tooth crown height were chosen for serial sampling. Each serial sample was obtained by drilling with a 1–2 mm-wide groove mostly perpendicular to the tooth growth axis, penetrating through the enamel layer's thickness at intervals of approximately 1–2 mm. These sampling methods were designed to encompass the full crown height of each tooth piece. Approximately 12–15 mg of enamel powder was drilled and collected in a 1.5-ml centrifuge tube for each sample.

Second, all the enamel powder underwent pretreatment with 2.5% NaOCl followed by 1 mol/L acetic acid. Subsequently, 3–5 mg of powdered enamel was analyzed at the Laboratory for Stable Isotope Geochemistry, Institute of Geology and Geophysics, Chinese Academy of Sciences using a MAT253 IRMS coupled with a Gasbench unit. The international isotope standards of IAEA CO-8 and NBS-19 were interspersed with every run to establish the standard curve for isotopic calibration. Additionally, the in-house standard GBW04405 (limestone) and sample replicates were analyzed to monitor measurement uncertainty. Carbon and oxygen isotope values were expressed as δ^{13}C and δ^{18}O values relative to VPDB. The analytical precision, based on long-term repeated measurements of the standards and sample replicates, was less than ± 0.15‰ for δ^{13}C values and ± 0.20‰ for δ^{18}O values.

Assessment of fossil tooth preservation in the Longdan fauna, as established in previous studies (Biasatti et al., 2010; Ma et al., 2023), suggests that the specimens in this study from the same fauna and sediments are likely well preserved.

3.4 Data analyses

We utilized the carbon isotope enrichment factors proposed in the most recent study based on modern animal experiments (Cerling et al., 2021): 13.5‰ for non-coprophagous hindgut fermenter (such as equids, woolly rhinoceroses, and mammoths) and 14.5‰ for ruminant foregut fermenter (including cervids, gazelles, and bovids). For the collagen samples from the Late Pleistocene, we applied 5‰ as the isotope enrichment factor (Cerling and Harris, 1999).

The isotopic data collected from different sites in this study cover a range of regions, necessitating the consideration of factors such as latitude and altitude. Previous studies have identified a positive relationship between elevation and the $\delta^{13}C$ values of C_3 plants, possibly influenced by air pressure and temperature (Körner et al., 1991; Männel et al., 2007). Conversely, the latitudinal gradient for the $\delta^{13}C$ values remains less definitive (Krajcarz et al., 2016). The positive correlation between elevation and the $\delta^{13}C$ values of C_3 plants has been noted in the modern Tibetan region as well (Wang et al., 2008b), which is pertinent to our studied locations. However, the relationship between $\delta^{13}C$ values of C_4 plants and the elevation gradients is unclear and may exhibit a negative correlation in the modern Tibetan region (Wang et al., 2008b). Additionally, no clear relationship was observed between $\delta^{18}O$ values of precipitation and altitude in this region (Wang et al., 2008b).

Therefore, the relationship between $\delta^{13}C$ values of C_3 plants and altitude appears to be an important factor in this study when analyzing isotopic values across sites at different elevations. We adopted the altitude gradient as per Männel et al. (2007): $\delta^{13}C$-adj-alt= $\delta^{13}C$ -(0.0011×altitude), where altitude in meters. By applying this correction, we mitigate the impact of altitude, normalizing all data to sea level (0 meter above sea level, asl) for comparability. However, due to the unclear association between $\delta^{13}C$ values of C_4 plants and elevation, we chose not to adjust data from the regions where C_4 plant components were notably present.

Mann-Whitney U tests were conducted to assess statistical variations in isotopic values across distinct groups. These analyses were conducted in PAST 4.03 (Hammer et al., 2001). Data visualizations were created in EXCEL and RStudio (RStudio Team, 2016) using ggplot2 (Wickham, 2011) and ggpubr (Kassambara, 2020).

4 Results and interpretations

4.1 Bulk carbon and oxygen isotope analyses

The $\delta^{13}C$ and $\delta^{18}O$ values for each tooth sample (bulk samples and the mean values of each serial sample) are summarized in Table 1 and displayed in Figure 1 (see original data in Supplementary Table S1). In order to capture a complete paleoecological scenario of the Longdan fauna, our previous data of the *E. eisenmannae* and *P. sinense* were also included (Ma et al., 2023). Overall, the $\delta^{13}C$ values of all the specimens in this study ranged from −13.3‰ to −7.9‰, and their $\delta^{18}O$ values ranged between −12.5‰ to −4.6‰. In Figure 1, $\delta^{13}C$ and $\delta^{18}O$ values of the Longdan equid samples were also fall into these ranges (Ma et al., 2023). This indicated that C_3 vegetation constituted a significant portion of the ungulates' diet and played a substantial role in the local environment during the Early Pleistocene in the Linxia Basin.

The $\delta^{13}C$ values of the four ungulates in this study were slightly lower than those of two equid species, which indicated that equids occupied more open environments than other mammals (Table 1; Figure 1). The results of the Mann-Whitney U tests revealed that the $\delta^{13}C$ values of *G. blacki* were lower than *P. sinense* and *E. eisenmannae* (p-values = 0.015, 0.009), suggesting a possible preference for close environments in *G. blacki* compared to equids. Overall, four ungulates analyzed in this study exhibited subtle differences in $\delta^{13}C$ values (Supplementary Table S2), indicating potential overlap in their food resources and habitats. The $\delta^{13}C$ standard deviation was higher for *C. nihowanensis* specimens in comparison to other mammals (Table 1), indicating the diverse habitats they inhabited. In a previous study, one *C. nihowanensis* specimen with a $\delta^{13}C$ value of −9.9‰ was classified as a grazer (Biasatti et al., 2018), within the range of $\delta^{13}C$ values observed in our *C. nihowanensis* specimens (from −13.3‰ to −8.8‰, n=7).

As shown in Table 1, the mean $\delta^{18}O$ values of the *G. blacki* and *N. longdanensis* specimens were higher than those of Bovinae and *E. eisenmannae* specimens, whereas the specimens of *C. nihowanensis* and *P. sinense* exhibited intermediate $\delta^{18}O$ values. The results from the Mann-Whitney U tests revealed that the $\delta^{18}O$ values of *E. eisenmannae* were lower than those of *N. longdanensis* and *C. nihowanensis* (refer to Supplementary Table S3), with no discernible differences were observed in other groups. This suggested that *E. eisenmannae* specimens likely rely more heavily on meteoric water resources (Sponheimer and Lee-Thorp, 1999), while *N. longdanensis* and *C. nihowanensis* may access different water resources, potentially obtaining a portion of their water from tree leaves. In general, tree leaves exhibit higher $\delta^{18}O$ values than grasses because trees experience greater transpiration of water through the leaves (Koch et al., 1989; Quade et al., 1995).

TABLE 1 Summary of the $\delta^{13}C$ and $\delta^{18}O$ values of the Longdan mammalian tooth enamel samples.

Taxon	N	$\delta^{13}C$/‰	SD	$\delta^{18}O$/‰	SD
C. nihowanensis	7	−10.9	1.6	−8.6	0.9
Bovinae	7	−10.4	1.2	−9.9	2.1
N. longdanensis	4	−10.9	1.1	−7.5	0.9
G. blacki	9	−11.4	0.9	−7.9	2.2
P. sinense	4	−9.5	1.0	−8.6	1.1
E. eisenmannae	8	−10.0	0.9	−9.8	0.7

These data were derived from bulk samples and the mean value of each serial sample. Data for *P. sinense* and *E. eisenmannae* are sourced from Ma et al. (2023); all other data are from this study. N represents the number of tooth samples, and SD denotes standard deviation.
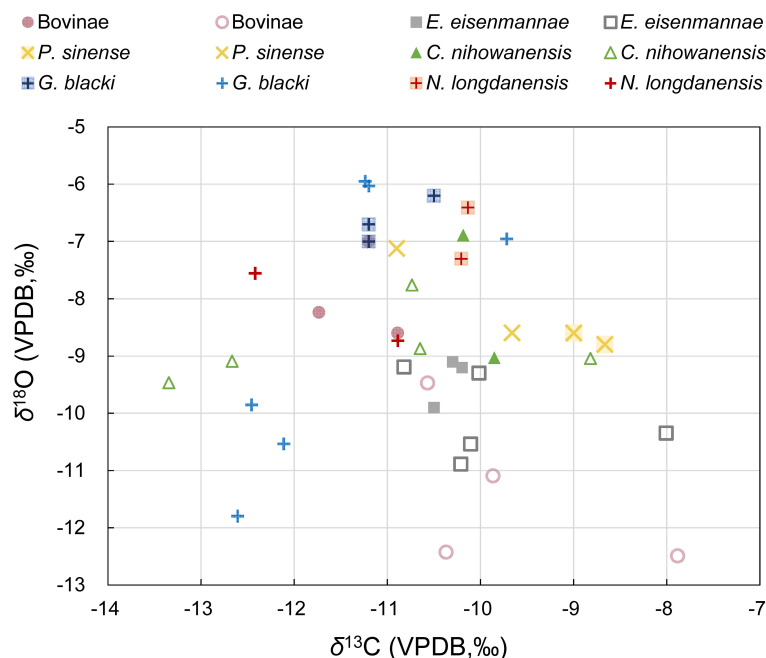
FIGURE 1
Stable isotopic data of the bulk samples (blank symbols) and the mean value of each serial sample (solid symbols) of the studied mammals (including data of *P. sinense* and *E. eisenmannae* from Ma et al., 2023).

Meanwhile, high standard deviations in $\delta^{18}O$ values were observed in the specimens of Bovinae, *G. blacki*, and *P. sinense*, suggesting potential access to a diverse range of water resources (Table 1; Figure 1). Nevertheless, these varied $\delta^{18}O$ values may be caused by the potential differences in the chronology of these specimens.

A discrepancy was noted in the isotopic results between the averaged serial samples and the bulk samples from the specimens of *N. longdanensis*, *P. sinense*, and Bovinae. This difference could be linked to potential sampling bias inherent in the two distinct sampling methods. Despite the bulk samples being designed to encompass the entire height of the tooth, challenges arise when dealing with fragmented or heavily worn teeth. Consequently, the stable isotopic values obtained from partial tooth heights could introduce bias and fail to accurately reflect the averaged isotopic values. Nevertheless, considering the subtle intra-tooth isotopic ranges in these serial samples, we propose that the data disparity probably reflects their varied isotopic ecologies. Furthermore, the potential differences in chronology could be another contributing factor to this data discrepancy, given the absence of precise stratigraphic levels for these tooth specimens.

4.2 Serial isotopic analysis

The serial isotopic patterns observed in these mammals indicated notable signals of the ecological and environmental seasonality. All eight fossil teeth examined in this study exhibited stable $\delta^{13}C$ values, with intra-tooth $\delta^{13}C$ values ranging from 0.8‰ to 1.6‰ (Supplementary Table S1). This possibly indicated limited seasonal variations in the local vegetation. By comparison, the serial

$\delta^{18}O$ profiles of these ungulates displayed interspecific differences (Figure 2). The intra-tooth $\delta^{18}O$ profiles of the large Bovinae (Supplementary Table S1; Figure 2) and equids (Biasatti et al., 2010; Ma et al., 2023) specimens demonstrated stable and monotonous patterns. The seasonal $\delta^{18}O$ values observed in these large obligate drinkers may have been dampened due to their frequent consumption of water from large water bodies, which mitigated seasonal isotopic variations in local rainfall, owning to prolonged water residence times (Roberts et al., 2018; Pederzani and Britton, 2019). Alternatively, the stability and monotony observed in the intra-tooth $\delta^{18}O$ profiles of the equid and bovid specimens might suggest migratory behavior. Consequently, their $\delta^{18}O$ values may reflect a combination of water sources from various locations.

The intra-tooth $\delta^{18}O$ ranges of three *G. blacki* specimens were 3.5‰, 3.5‰, and 4.8‰, exhibiting greater variability compared to those of the Bovinae (1.7‰, 1.3‰, and 1.4‰) and *C. nihowanensis* (1.7‰, 2.1‰) specimens. The intra-tooth $\delta^{18}O$ ranges of the *C. nihowanensis* specimens were slightly larger than those of the Bovinae specimens in this study and equid specimens (0.7‰, 1.4‰, 1.5‰, and 2.3‰) in Ma et al. (2023). Regular sinusoidal patterns were observed in the serial $\delta^{18}O$ profiles of the *C. nihowanensis* specimens (Figure 2). This suggested that *C. nihowanensis* specimens possibly obtain fewer water resources from the longstanding water bodies, unlike the large Bovinae and equids (Biasatti et al., 2010; Ma et al., 2023). The distinct water resources of the *C. nihowanensis* specimens, compared to the Bovinae and equids, previously inferred from their higher $\delta^{18}O$ values (Table 1; Supplementary Table S3), were consistent with this finding inferred from the different serial isotopic profiles. Alternatively, *C. nihowanensis* specimens might be non-migratory
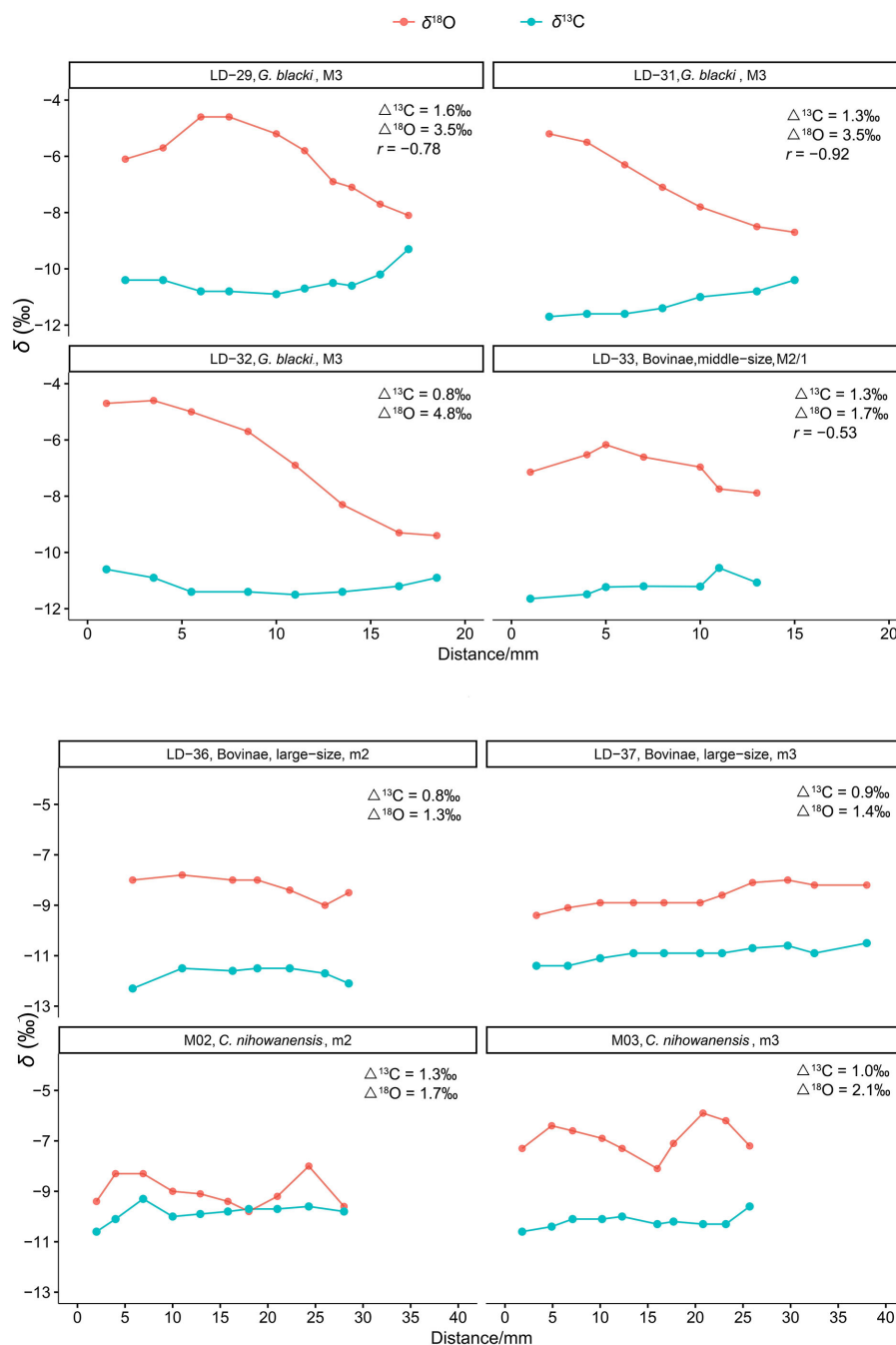
FIGURE 2
Serial isotopic profiles of the fossil mammals in this study. (Δ^{13}C and Δ^{18}O are the ranges of the intra-tooth δ^{13}C and δ^{18}O values).

and thus could record the δ^{18}O signals of local environments for more than one year (Figure 2).

Furthermore, an inverse relationship between the intra-tooth δ^{13}C and δ^{18}O values were observed for two *G. blacki* specimens (LD-29, 31; $r =-0.78$, -0.92) and one middle-sized Bovinae specimen (LD-33, $r =-0.53$).

In Supplementary Figure S1, we plotted the serial isotope profiles of two modern goats from the different regions in the Linxia Basin and its vicinity with varying altitudes. The average δ^{13}C values of these two samples were -10.1 ± 2.8‰ (n=6) and -11.9 ± 0.9‰ (n=5),

respectively; and their mean δ^{18}O values were -5.2 ± 1.4‰ and -7.1 ± 1.9‰. The intra-tooth range of δ^{13}C values for one goat specimen was higher, and its serial δ^{13}C values ranged from -13.4‰ to -6.3‰, clearly indicating seasonal C_4 food resources. The intra-tooth δ^{18}O ranges of these two goats were 4.5‰ and 3.6‰, slightly higher than those of three fossil *G. blacki* specimens. Additionally, inverse relationships between δ^{13}C and δ^{18}O values were observed for both goat specimens ($r = -0.83$, -0.86).

The isotopic results of the modern goats indicated the occurrence of East Asia Summer Monsoon (EASM) and the presence of seasonal

C_4 plants. For both specimens, the peaks of $\delta^{13}C$ values indicated the ingestion of C_4 plants during the summer, and their corresponding $\delta^{18}O$ values were the lowest. In a monsoonal region, the "amount effect" affects seasonal $\delta^{18}O$ values of precipitation, preferentially removing ^{18}O from vapor, resulting in lower $\delta^{18}O$ values in summer (Dansgaard, 1964; Rozanski et al., 1993). High precipitation and warm temperatures favor C_4 plants, which are naturally more abundant in summer. Therefore, an inverse relationship between $\delta^{13}C$ and $\delta^{18}O$ values is expected (Higgins and MacFadden, 2004; Wang et al., 2008b; Biasatti et al., 2010; Yang et al., 2012; Zhang et al., 2012; Ciner et al., 2015).

In Figure 2 and Supplementary Figure S1, the serial isotopic profiles of the two modern goats were similar to those of a part of fossil teeth in this study, especially the *G. blacki* specimens. Through these modern references, this study provides evidence once again that the EASM occurred in the Linxia Basin during the Early Pleistocene (Biasatti et al., 2010). Furthermore, it appears that non-obligate drinkers offer better indicators of seasonal variations in local environments than large obligate drinkers (Roberts et al., 2018; Pederzani and Britton, 2019; Hodgkins et al., 2020).

Based on this and previous studies (Wang and Deng, 2005; Biasatti et al., 2010; Ma et al., 2023), the paleoenvironment in the Linxia Basin, as inferred from mammalian carbon isotopes during the Early Pleistocene was primarily characterized by C_3 plants, with C_4 plants likely representing a minor component that was seasonally consumed by the studied mammals. This finding aligns with the isotopic results of the carbonates from fluvial and lacustrine sediments (Dettman et al., 2003; Hough et al., 2011). The sub-humid climate and the occurrence of EASM are further supported by previous studies, including stable isotope analysis (Biasatti et al., 2010), fossil assemblage analysis (Qiu et al., 2002; Wang, 2005; Xue et al., 2006), and sedimentary analysis (Zan et al., 2016).

5 Discussion

5.1 Foraging ecologies and environmental contexts of *C. nihowanensis* in Early Pleistocene northern China

Studying the foraging ecologies of *C. nihowanensis* in northern China from west to east can provide valuable insights into the relationship between their ecological behaviors and paleoenvironments during the Early Pleistocene. This study provides a comprehensive insight into the paleoecology of the earliest *C. nihowanensis* in northwestern China, situated on the edge of the Tibetan Plateau. Within the Linxia Basin, *C. nihowanensis* specimens were likely a mixed feeder inhabiting diverse habitats, as indicated by their wide distribution of the $\delta^{13}C$ values and intermediate $\delta^{18}O$ values compared to other coexisted mammals. Meanwhile, recent stable isotopic studies on mammalian faunas in the Nihewan Basin aiming to explore the paleoenvironmental settings of early humans can serve as a strong evidence for the paleoecology of *C. nihowanensis* in eastern China (Xu et al., 2021; Xu et al., 2023). Therefore, it is a great chance to compile all these data and explore the paleoecological changes of the

C. nihowanensis (Figure 3; Supplementary Table S4). Besides, the same pretreatment methods of the stable isotopic analysis for these two faunas in the same laboratory could guarantee the validity of the cross comparison. Considering the potential bias in $\delta^{18}O$ values stemmed from variations in phosphoric acid reaction temperatures (Passey et al., 2007) during the isotopic measurements conducted in different laboratories, the isotopic data from Wang and Deng (2005) as well as Biasatti et al. (2010, 2018) were deliberately not included in Figure 3. It is worth noting, however, that the intra-tooth isotopic ranges from these studies have been collated and are presented in Figure 4 (Supplementary Table S5). The altitude of the Linxia and Nihewan basins during the Early Pleistocene were already situated at their current elevations and therefore, $\delta^{13}C_{diet}$ values were corrected with the modern altitudes of 2248 m and ~940 m (Deng et al., 2013; Pei et al., 2019), respectively. $\delta^{13}C_{diet}$-adj-alt were corrected using the formula described in section 3.4. This correction was applied at the Longdan and Shanshenmiaozui sites, where the ungulates' diets predominantly consisted of almost pure C_3 plants. However, in light of the significant components of the C_4 plants in the diet of these ungulates, this correction was not applied in other three sites during ca. 1.2–1.1 Ma in the Nihewan Basin.

Among the four sites in the Nihewan Basin, Shanshenmiaozui has yielded the richest mammalian fossils. Based on the analysis of the faunal assemblage, the age of the Shanshenmiaozui fauna likely corresponds closely with the classic Nihewan fauna during the early Early Pleistocene, with an approximate age of 2.2–1.7 Ma (Tong et al., 2021). The other three sites–Madigou, Donggutuo, and Feiliang–are classified as Early Paleolithic, with the age of ca. 1.2–1.1 Ma, late Early Pleistocene (Wang et al., 2005; Deng et al., 2007; Pei et al., 2019).

In Figure 3, the $\delta^{13}C_{diet}$-adj-alt values of the Shanshenmiaozui fauna (−25.9± 1.6‰, n=65) were higher than those of the Longdan fauna (−27.1± 1.4‰, n=39) (*p*-value of Mann-Whitney *U* test: 0.0005) (Ma et al., 2023; Xu et al., 2023; this study). However, such variation may not be directly linked to the difference in landscape between these two sites (Negash and Barr, 2023). The $\delta^{18}O$ values of the Shanshenmiaozui fauna (−9.8± 1.4‰, n=65) were slightly lower than those of the Longdan fauna (−8.8± 1.7‰, n=39) (*p*-value of Mann-Whitney *U* test: 0.001), possibly indicating a wetter and/or more humid environment in the Nihewan Basin during the early Early Pleistocene (Ma et al., 2023; Xu et al., 2023; this study).

The intra-tooth $\delta^{13}C$ and $\delta^{18}O$ ranges of the single equid specimen in Shanshenmiaozui were higher than those of the Longdan equid specimens (Figure 4) (Biasatti et al., 2010; Ma et al., 2023; Xu et al., 2023; this study). This might suggest a more pronounced climatic seasonality in the Nihewan Basin compared to the Linxia Basin, despite the limited serial sample amount in Shanshenmiaozui. Nonetheless, it seems that C_4 grasses may not have become a significant component of the local ecosystems in the Nihewan Basin during this period.

In the Shanshenmiaozui fauna, *C. nihowanensis* and bovids exhibited intermediate $\delta^{13}C_{diet}$-adj-alt values, which were lower than those of equids but higher than cervid ones (Figure 3; Supplementary Table S6) (Xu et al., 2023). This indicated that *C. nihowanensis* and bovid specimens in Shanshenmiaozui likely inhabited mixed grasslands and woodlands. Statistical analyses
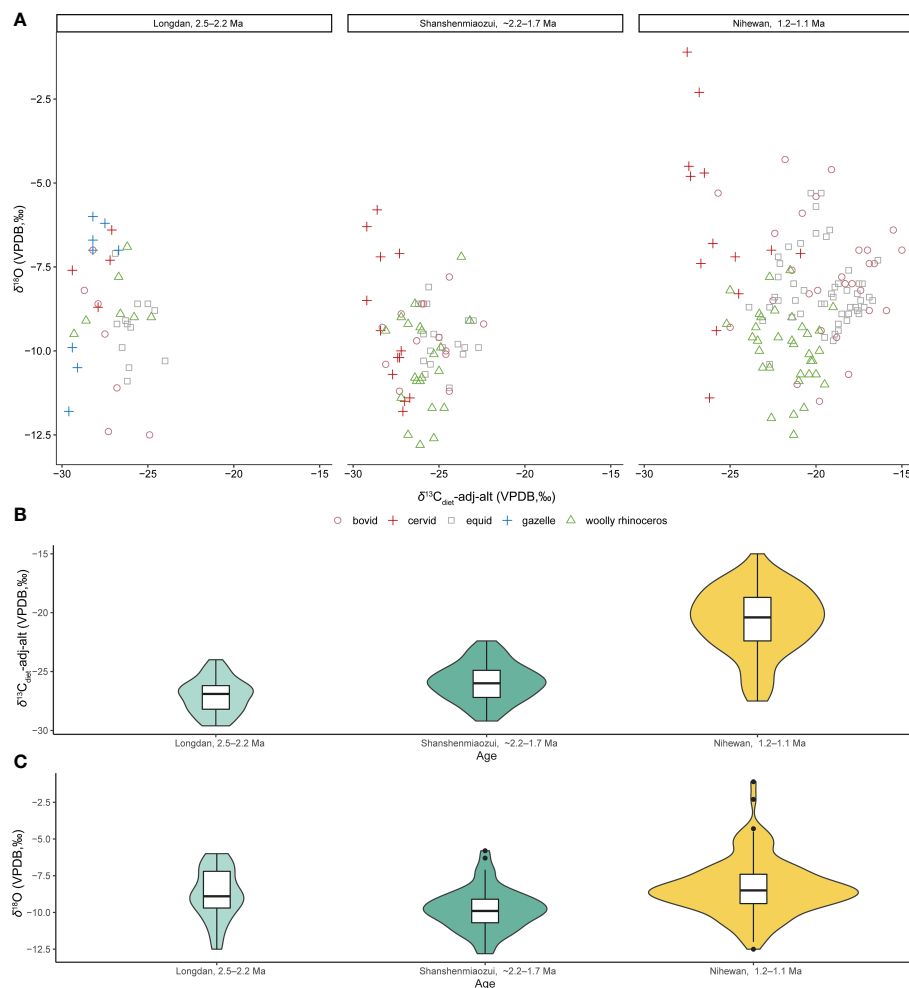
FIGURE 3
$\delta^{13}C_{diet}$-adj-alt and $\delta^{18}O$ values of the Longdan fauna and Nihewan fauna (~2.2–1.7 Ma: Shanshenmiaozu; ca. 1.2–1.1 Ma: Madigou, Feiliang, and Donggutuo) (Xu et al., 2021, 2023; Ma et al., 2023; this study) (Supplementary Table S4). **(A)** Scatter plot of $\delta^{13}C_{diet}$-adj-alt and $\delta^{18}O$ values of different taxa. **(B)** Violin plot and boxplot of $\delta^{13}C_{diet}$-adj-alt values of all the mammalian species. **(C)** Violin plot and boxplot of $\delta^{18}O$ values of all the mammalian species. (These data consist of bulk samples and the mean values of each serial sample. For panels B and C, the width of the "violin" at a particular value reflects the data density at that point. Within the boxplot, the lower hinge, median line, and upper hinge denote the 25th percentile, median, and the 75th percentile, respectively. The lower whisker extends to the smallest observation at or above the first quartile (Q1) minus 1.5 times the Interquartile Range (IQR), while the upper whisker extends to the largest observation at or below the third quartile (Q3) plus 1.5 times the IQR. The potential outliers in the dataset are marked by separate points).

displayed no differences in the $\delta^{18}O$ values among these groups (Supplementary Table S7). However, $\delta^{18}O$ values were lowest for *C. nihowanensis* among all the coexisting mammals (Figure 3), possibly indicating that these specimens obtained abundant meteoric water and possibly inhabit areas close to lakes and/or rivers (Xu et al., 2023).

Until the late Early Pleistocene, the mean $\delta^{13}C_{diet}$-adj-alt and $\delta^{18}O$ values of the three sites during ca. 1.2–1.1 Ma were higher than those of the Shanshenmiaozui fauna (*p*-values of Mann-Whitney *U* tests for $\delta^{13}C$ and $\delta^{18}O$: 0.0005, 0.0001) (Figure 3) (Xu et al., 2021; Xu et al., 2023). This indicated that the C_4 vegetation became significant in the Nihewan Basin during the late Early Pleistocene. The intra-tooth ranges in $\delta^{13}C$ and $\delta^{18}O$ values of the equid and bovid specimens at these three sites were greater than those of the Longdan and Shanshenmiaozui specimens (Figure 4; Supplementary Table S5) (Biasatti et al., 2010; Xu et al., 2021; Ma

et al., 2023; Xu et al., 2023; this study), possibly indicating seasonal ingestion of a substantial amount of C_4 plants in their diets and more pronounced seasonal fluctuations in precipitation. An inverse relationship between $\delta^{13}C$ and $\delta^{18}O$ values was observed in some serial equid and bovid specimens in Donggutuo and Feiliang sites (Supplementary Table S5) (Xu et al., 2023), which was the signal of the EASM as aforementioned. Therefore, the paleoenvironments in the Nihewan Basin during the late Early Pleistocene were possibly varied and experienced pronounced seasonality under the effect of intensive EASM and the winter monsoon (Xu et al., 2021; Xu et al., 2023).

The $\delta^{13}C_{diet}$-adj-alt values of the *C. nihowanensis* specimens during ca. 1.2–1.1 Ma were also lower than those of equid and bovid specimens but higher than cervid ones (Figure 3; Supplementary Table S8) (Xu et al., 2021; Xu et al., 2023), indicating that *C. nihowanensis* specimens fed on mixed C_3/C_4 vegetation, and
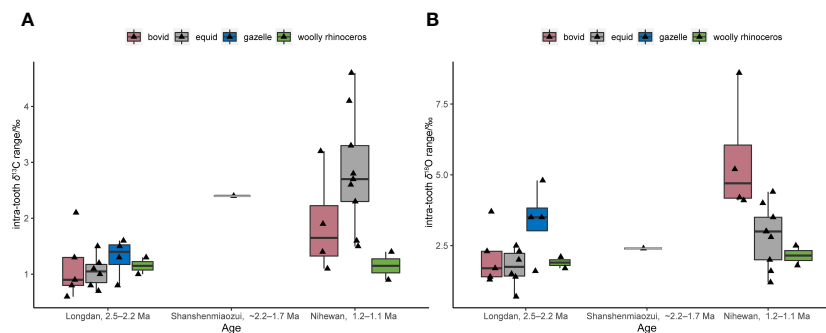
FIGURE 4
Intra-tooth δ^{13}C **(A)** and δ^{18}O ranges **(B)** of the serial samples in the Linxia Basin (Longdan) and Nihewan Basin (Shanshenmiaozu, ~2.2–1.7 Ma; Madigou, Feiliang, and Donggutuo are ca. 1.2–1.1 Ma) (Biasatti et al., 2010; Xu et al., 2021, 2023; Ma et al., 2023; this study) (Supplementary Table S5). (The boxplot conveys the same meaning as Figure 3, but without annotating the outliers to avoid redundancy with the original data points represented by the jitter scatter plot).

consumed less C$_4$ grasses than equids and bovids. Furthermore, *C. nihowanensis* specimens exhibited the lowest δ^{18}O values (Figure 3; Supplementary Table S9), and the intra-tooth ranges in δ^{13}C and δ^{18}O values of *C. nihowanensis* were found to be smaller than those of the equids and bovids (Figure 4; Supplementary Table S5) (Xu et al., 2021; Xu et al., 2023). This possibly indicated that *C. nihowanensis* occupied relatively close and well-watered environments which experienced fewer seasonal changes. Therefore, *C. nihowanensis* in the Nihewan Basin during the late Early Pleistocene was likely a mixed feeder and showed a preference for close environments (Xu et al., 2021; Xu et al., 2023).

During the early Early Pleistocene, the paleoenvironments in the Linxia and Nihewan basins were primarily dominated by C$_3$ vegetation, with the latter likely exhibited a stronger EASM compared to the Linxia Basin. Previous studies found that C$_4$ signals were more abundant in the Linxia Basin at ~1.2 Ma (Wang and Deng, 2005; Biasatti et al., 2010). The increasing prevalence of C$_4$ plants and a pronounced EASM in the Linxia and Nihewan basins around 1.2–1.1 Ma potentially aligns with the widespread aridification in northern China (Da et al., 2015; Zhou et al., 2018). Against this backdrop, *C. nihowanensis* owned a notable dietary flexibility and were able to thrive in a variety of environments across northern China from west to east throughout the Early Pleistocene. Such ecological adaptability of *C. nihowanensis* is presumed to have been influenced by the intricate terrain of Early Pleistocene East Asia and its diverse environments, which were situated along the migration path of the woolly rhinoceroses from the Tibetan Plateau to northern Eurasia.
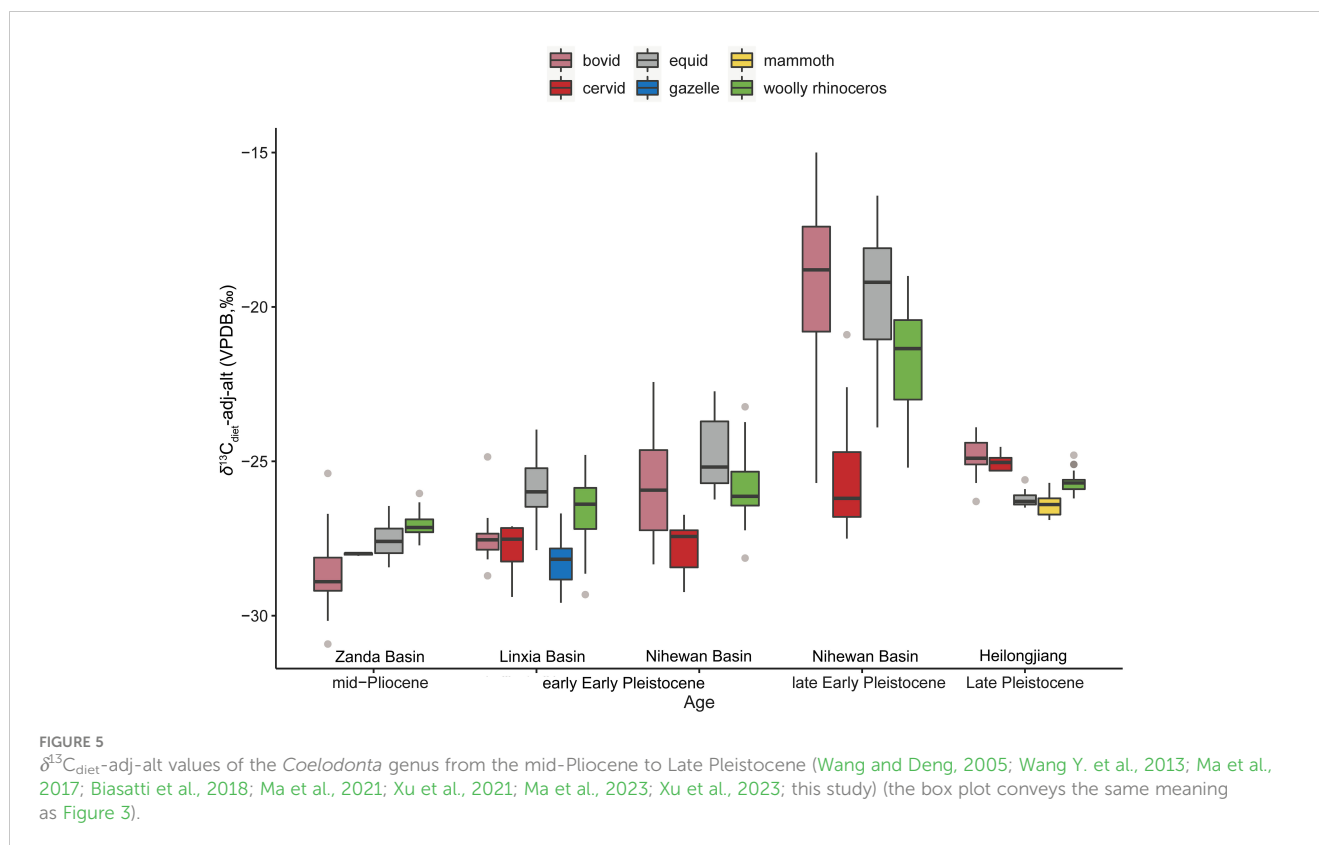
5.2 Ecological adaptation of *Coelodonta* and coexisting mammals

After thoroughly examining the isotopic paleoecology of *C. nihowanensis* in Early Pleistocene East Asia, it is imperative to delve deeper into the paleoecology of its ancestral and derived species to capture the paleoecological evolution of *Coelodonta*. We complied all δ^{13}C$_{diet}$-adj-alt values of the *Coelodonta* genus and other coexisting mammals in East Asia from the mid-Pliocene to

Late Pleistocene in Figure 5 (Supplementary Table S4). During the mid-Pliocene, it was estimated that the elevation of the Zanda Basin was similar to its modern altitude, approximately 4,000 meters asl (Deng et al., 2012). Given that the modern altitudes of these Late Pleistocene sites were around 100–200 meters, it is assumed that the altitude effect could be disregarded in this context.

During the mid-Pliocene, the δ^{13}C$_{diet}$-adj-alt values of *C. thibetana* in the Zanda Basin ranged narrowly between −27.7‰ to −26.0‰ (n=22), with their mean δ^{13}C$_{diet}$-adj-alt (−27.0± 0.4‰) being higher than those of the bovid (−28.6± 1.3‰, n=19), equid (−27.6± 0.5‰, n=30), and cervid (−28.0± 0.1‰, n=3) specimens (Supplementary Table S10; Figure 5) (Wang Y. et al., 2013). Additionally, both carbon and oxygen isotopes of the *C. thibetana* specimens showed lower standard deviations than those of the bovids and equids (Figure 5; Wang Y. et al., 2013). This suggested that the ancestral *C. thibetana* primarily fed on C$_3$ grasses and occupied a confined ecological niche in open environments at the high-altitude Zanda Basin. *C. thibetana* occupies the most basal position of the *Coelodonta* lineage and was considered the earliest representative of this genus (Deng et al., 2011). The morphological traits of the *C. thibetana*, such as the highly elongated skull, large and roughened nasal horn base, and high tooth crowns with rough enamel, are indicative of an adaptation to efficiently graze in cold and arid environments. These were in consistent with its foraging ecology inferred from stable isotopes.

C. thibetana moved down from the Tibetan Plateau toward northeastern Linxia Basin (~2,500 m asl) at the initiation of the Quaternary and evolved as *C. nihowanensis*. The average δ^{13}C$_{diet}$-adj-alt value of the Longdan fauna (−26.9± 1.4‰, n=55) (Wang and Deng, 2005; Biasatti et al., 2018; Ma et al., 2023; this study) was higher than that of the Zanda fauna (−27.7± 1.0‰, n=74) (*p*-value of Mann-Whitney *U* test: 0.0008) (Wang Y. et al., 2013), possibly indicating a drier/warmer climate in the Early Pleistocene Linxia Basin. The broader range of δ^{13}C$_{diet}$-adj-alt values observed in the *C. nihowanensis* specimens in the Linxia Basin (Biasatti et al., 2018; this study) compared to coexisting mammals, in contrast to the narrower range of the δ^{13}C$_{diet}$-adj-alt values seen in the ancestral *C. thibetana* in the Zanda fauna, suggested that *C. nihowanensis* diversified its ecological niche during this period. In the Zanda and

FIGURE 5
$\delta^{13}C_{diet}$-adj-alt values of the *Coelodonta* genus from the mid-Pliocene to Late Pleistocene (Wang and Deng, 2005; Wang Y. et al., 2013; Ma et al., 2017; Biasatti et al., 2018; Ma et al., 2021; Xu et al., 2021; Ma et al., 2023; Xu et al., 2023; this study) (the box plot conveys the same meaning as Figure 3).

Longdan faunas, both woolly rhinoceroses and equids had higher $\delta^{13}C_{diet}$-adj-alt values than those of artiodactyls (Figure 5) (Wang Y. et al., 2013), suggesting a possible ecological niche partitioning between artiodactyls and perissodactyls.

In Section 5.1, a thorough discussion has been conducted on the paleoenvironmental and paleoclimatic changes in the Nihewan Basin during the Early Pleistocene. In the Shanshenmiaozui fauna, equids occupied open grasslands and exhibited the highest $\delta^{13}C_{diet}$-adj-alt values (-24.8 ± 1.1‰, n=18) among all the mammalian species (Supplementary Table S6) (Xu et al., 2023). Similar $\delta^{13}C_{diet}$-adj-alt values were observed for woolly rhinoceroses (-25.9 ± 1.2‰, n=21) and bovids (-25.7 ± 1.7‰, n=13) in this fauna (Supplementary Table S6), indicating similar habitat preferences for both species (Xu et al., 2023). The lowest $\delta^{13}C_{diet}$-adj-alt values (-27.8 ± 0.8‰, n=13) of the cervid specimens reflected a preference for browsing in a more close environment (Supplementary Table S6) (Xu et al., 2023). Therefore, *C. nihowanensis* and bovids in Shanshenmiaozui were possibly mixed feeders and likely inhabited relatively open environments in Shanshenmiaozui. These ecological niches within the Shanshenmiaozui fauna inferred from the $\delta^{13}C_{diet}$-adj-alt values were similar to the pattern observed in the Longdan fauna.

In the Feiliang, Madigou, and Donggutuo sites, bovids and equids exhibited much higher $\delta^{13}C_{diet}$-adj-alt values (-19.3 ± 2.6‰, n=29; -19.6 ± 1.9‰, n=51) than those of the woolly rhinoceroses (-21.7 ± 1.6‰, n=34) and cervids (-25.6 ± 2.0‰, n=13) (refer to Supplementary Table S8) (Xu et al., 2021; Xu et al., 2023). This suggested that the former consumed a greater amount of C_4 grasses and inhabited more open environments compared to the latter during

the late Early Pleistocene. *C. nihowanensis* likely had a mixed diet and favored a relatively close habitat during ca. 1.2–1.1 Ma. This contrasted slightly with the preference for open environments observed in earlier *C. nihowanensis* specimens from Shanshenmiaozui within the same region. Consequently, it seems that *C. nihowanensis* in the Nihewan Basin displayed varying ecological preferences during different periods of the Early Pleistocene.

The ecological niche partitioning among these mammalian taxa during the late Early Pleistocene differed from the pattern observed in previous faunas, indicating notable ecological shifts among these mammalian taxa in eastern China. Throughout the mid-Pliocene to late Early Pleistocene, equids consistently favored open environments, reflecting a grazing preference similar to their modern counterparts (Ransom and Kaczensky, 2016). Within the Nihewan Basin, bovids exhibited a highly diverse foraging ecology, gradually expanding into open environments compared to the Zanda and Linxia basins (Xu et al., 2021; Xu et al., 2023). However, the habitats of the *C. nihowanensis* slightly shifted towards more close environments in the Nihewan Basin (Xu et al., 2021; Xu et al., 2023). This suggested distinct foraging strategies between bovids and woolly rhinoceroses in response to changing paleoenvironments.

C. nihowanensis is estimated to have a larger body size (approximately 1700 kg according to the NOW database[1]) compared to the ancestral *C. thibetana* (~1470 kg[1]), and its

---

1 The NOW Community. New and Old Worlds Database of Fossil Mammals (NOW). Licensed under CC BY 4.0. https://nowdatabase.org/now/database/.

morphological traits were also considered as a grazing adaptation in cold and dry environments. However, the foraging ecologies of *C. nihowanensis* were more flexible and even displayed a preference for close environments. Additionally, the limb bones of *C. nihowanensis* are more slender than those of the derived *C. tologoijensis*, indicating a better running ability (Deng, 2008). However, the isotopic results of the *C. nihowanensis* specimens from both Linxia and Nihewan basins likely exhibited a potential of non-migratory behaviors as aforementioned. This highlights the distinction between individual behavioral selection and population dispersal as well as evolutionary history.

C. tologoijensis (~2000 kg[1]) has a remarkably larger body size than the primary *C. nihowanensis*, and its paleoecology was rarely explored. According to the paleoenvironmental records of the sites in Asia which preserved *C. tologoijensis* fossils, Kahlke and Lacombat (2008) presumed that *C. tologoijensis* possibly inhabited meadow to forest steppes, similar to those found in northern Mongolia today.

C. antiquitatis first occurred during the late Middle Pleistocene and thrived in northern Eurasia during the Late Pleistocene as an emblematic member in the *Mammuthus-Coelodonta* Faunal Complex, and its paleoecology was intensively explored. *C. antiquitatis* was graviportal and has a massive body size (~2900 kg[1]), as a highly progressive species of *Coelodonta* (Boeskorov, 2001; Stuart and Lister, 2012). A series of anatomical features observed in *C. antiquitatis*, including wide lips, low posture of the head, long nasal horn, high tooth crown, long hair, and dense underwool, all indicating an adaptation for grazing in dry and frosty environments (Kahlke and Lacombat, 2008; Boeskorov et al., 2011b; Boeskorov, 2012).

The increasing number of paleoecological studies using multiple methods has revealed that *C. antiquitatis* from the northern Eurasia was a typical grazer with a highly abrasive diet, including dental microwear and mesowear analyses (Rivals et al., 2010; Rivals and Lister, 2016; Rivals and Álvarez-Lao, 2018; Pushkina et al., 2020), stable isotope analysis (e.g. Bocherens et al., 1991; Bocherens et al., 1997; Pushkina et al., 2014; Schwartz-Narbonne et al., 2019), and the examination of plant remains from gastro-intestinal content (Boeskorov et al., 2011a; Stefaniak et al., 2021) and teeth (van Geel et al., 2019; Stefaniak et al., 2021). Nonetheless, some studies have indicated a more mixed diet, signifying dietary plasticity and seasonality of *C. antiquitatis* (Rivals et al., 2010; Tiunov and Kirillova, 2010; Rivals and Lister, 2016; Rey-Iglesia et al., 2021).

The stable carbon and nitrogen isotope analyses of the *Mammuthus-Coelodonta* Faunal Complex in Heilongjiang suggested that *C. antiquitatis* may have been a grazer in East Asia, while also exhibiting dietary flexibility (as indicated by their intermediate $\delta^{13}C$ and relatively high $\delta^{15}N$ values, see Supplementary Tables S4, S11, S12; the isotopic pattern of the plants on the mammoth steppe was different from other biomes discussed here) (Ma et al., 2017; Ma et al., 2021). Within this fauna, delineation of ecological niche using carbon and nitrogen isotopic signatures roughly suggested a grazing ecology for mammoths, woolly rhinoceroses, and bovids, while equid specimens appear to have consumed more shrub or tree leaves, and cervid specimens likely ingested lichens, mosses, and leaves (Ma et al., 2017; Ma et al., 2021). This suggests that various taxa exhibited distinct ecological strategies when confronted with a completely distinct paleoenvironments during the Late Pleistocene.

The abundance and wide distribution of *C. antiquitatis* in Late Pleistocene East Asia have been well-documented (Tang et al., 2003; Li and Dong, 2007; Dong et al., 2014; Chen et al., 2016; Li et al., 2018). *C. antiquitatis* coexisted with woolly mammoths in northeastern China and the straight-tusk elephant *Palaeoloxodon* in warmer zones, with the southernmost boundary at 33° latitude (Tong, 2004; Tong et al., 2008; Dong et al., 2014; Wang et al., 2021). *Coelodonta-Palaeoloxodon* sympatry also occurred in England (Schreve, 2001, 2019). The faunal mixture and the wide distribution of *C. antiquitatis* may be linked to glacial/interglacial cycles, yet they also suggest the high ecological adaptability of *C. antiquitatis*, enabling this species to flourish in both cold and temperate environments.

This study conducted a comprehensive review of the paleoecological and evolutionary history of the woolly rhinoceroses from a spatiotemporal perspective. The ancestral *C. thibetana* and the terminating *C. antiquitatis* were more likely grazers that inhabited the high-altitude Tibetan Plateau during the mid-Pliocene and the middle to high latitude Eurasia during the Late Pleistocene. In contrast, *C. nihowanensis*, an intermediate form of the woolly rhinoceroses, exhibited flexible foraging ecologies across varied environments from west to east in northern China. The wide distribution of *C. antiquitatis* in temperate regions also indicates its high environmental tolerance. As an iconic cold-adapted mammal, *Coelodonta* adjusted its ecological strategies upon departing the Tibetan Plateau, ultimately dispersing from East Asia and colonizing middle to high latitude Eurasia. Further exploration of the paleoecology of the Middle Pleistocene *C. tologoijensis* will enhance our understanding of the complete ecological evolution of *Coelodonta*. While this paper reconstructed the paleoecology of the genus *Coelodonta* from an isotopic perspective, it is evident that further multidisciplinary investigations including systematic stratigraphy analysis, microwear and mesowear analyses, ecomorphological analysis, and locomotive behavior analysis are required to gain a more comprehensive understanding of the paleoecology of the ancestors of the woolly rhinoceroses.

Data availability statement

The original contributions presented in the study are included in the article/Supplementary Material. Further inquiries can be directed to the corresponding author.

Author contributions

JM: Conceptualization, Data curation, Funding acquisition, Investigation, Methodology, Writing – original draft, Writing –

Conflict of interest

The authors declare that the research was conducted in the absence of any commercial or financial relationships that could be construed as a potential conflict of interest.

Publisher's note

Supplementary material

The Supplementary Material for this article can be found online at: https://www.frontiersin.org/articles/10.3389/fevo.2024.1377000/full#supplementary-material

References

Ambrose, S. H., and Norr, L. (1993). "Experimental evidence for the relationship of the carbon isotope ratios of whole diet and dietary protein to those of bone collagen and carbonate," in *Prehistoric Human Bone*. Eds. Lambert, J. B., and Grupe, G. (Springer, Berlin, Heidelberg), 1–37.

Balasse, M. (2002). Reconstructing dietary and environmental history from enamel isotopic analysis: time resolution of intra-tooth sequential sampling. *Int. J. Osteoarchaeol.* 12, 155–165. doi: 10.1002/oa.601

Bender, M. M. (1968). Mass spectrometric studies of carbon 13 variations in corn and other grasses. *Radiocarbon* 10, 468–472. doi: 10.1017/S0033822200011103

Biasatti, D., Wang, Y., and Deng, T. (2010). Strengthening of the East Asian summer monsoon revealed by a shift in seasonal patterns in diet and climate after 2–3Ma in northwest China. *Palaeogeogr. Palaeoclimatol. Palaeoecol.* 297, 12–25. doi: 10.1016/j.palaeo.2010.07.005

Biasatti, D., Wang, Y., and Deng, T. (2018). Paleoecology of Cenozoic rhinos from northwest China: a stable isotope perspective. *Vertebr. Palasiat.* 56, 45–68. doi: 10.19615/j.cnki.1000-3118.170519

Blumenthal, S. A., Cerling, T. E., Chritz, K. L., Bromage, T. G., Kozdon, R., and Valley, J. W. (2014). Stable isotope time-series in mammalian teeth: *In situ* $\delta^{18}O$ from the innermost enamel layer. *Geochim. Cosmochim. Acta* 124, 223–236. doi: 10.1016/j.gca.2013.09.032

Blumenthal, S. A., Cerling, T. E., Smiley, T. M., Badgley, C. E., and Plummer, T. W. (2019). Isotopic records of climate seasonality in equid teeth. *Geochim. Cosmochim. Acta* 260, 329–348. doi: 10.1016/j.gca.2019.06.037

Bocherens, H., Billiou, D., Patou-Mathis, M., Bonjean, D., Otte, M., and Mariotti, A. (1997). Paleobiological implications of the isotopic signatures (^{13}C, ^{15}N) of fossil mammal collagen in Scladina Cave (Sclayn, Belgium). *Quat. Res.* 48, 370–380. doi: 10.1006/qres.1997.1927

Bocherens, H., Fizet, M., Mariotti, A., Lange-Badre, B., Vandermeersch, B., Borel, J. P., et al. (1991). Isotopic biogeochemistry ($^{13}C,^{15}N$) of fossil vertebrate collagen: application to the study of a past food web including Neandertal man. *J. Hum. Evol.* 20, 481–492. doi: 10.1016/0047-2484(91)90021-M

Boeskorov, G. G. (2001). Woolly rhino (*Coelodonta antiquitatis*) distribution in Northeast Asia. *Deinsea* 8, 15–20.

Boeskorov, G. G. (2012). Some specific morphological and ecological features of the fossil woolly rhinoceros (*Coelodonta antiquitatis* Blumenbach 1799). *Biol. Bull.* 39, 692–707. doi: 10.1134/S106235901208002X

Boeskorov, G. G., Bakulina, N. T., Davydov, S. P., Shchelchkova, M. V., and Solomonov, N. G. (2011a). Study of pollen and spores from the stomach of a fossil woolly rhinoceros found in the lower reaches of the Kolyma river. *Dokl. Biol. Sci.* 436, 23–25. doi: 10.1134/S0012496611010017

Boeskorov, G. G., Lazarev, P. A., Sher, A. V., Davydov, S. P., Bakulina, N. T., Shchelchkova, M. V., et al. (2011b). Woolly rhino discovery in the lower Kolyma River. *Quat. Sci. Rev.* 30, 2262–2272. doi: 10.1016/j.quascirev.2011.02.010

Bryant, J. D., and Froelich, P. N. (1995). A model of oxygen isotope fractionation in body water of large mammals. *Geochim. Cosmochim. Acta* 59, 4523–4537. doi: 10.1016/0016-7037(95)00250-4

Cerling, T. E., Bernasconi, S. M., Hofstetter, L. S., Jaggi, M., Wyss, F., Rudolf von Rohr, C., et al. (2021). CH_4/CO_2 ratios and carbon isotope enrichment between diet and breath in herbivorous mammals. *Front. Ecol. Evol.* 9, 638568. doi: 10.3389/fevo.2021.638568

Cerling, T. E., and Harris, J. M. (1999). Carbon isotope fractionation between diet and bioapatite in ungulate mammals and implications for ecological and paleoecological studies. *Oecologia* 120, 347–363. doi: 10.1007/s004420050868

Cerling, T. E., Harris, J. M., MacFadden, B. J., Leakey, M. G., Quade, J., Eisenmann, V., et al. (1997). Global vegetation change through the Miocene/Pliocene boundary. *Nature* 389, 153–158. doi: 10.1038/38229

Chen, J., Yin, Y. Q., li, T., and Jin, L. Y. (2016). The *Mammuthus-Coelodonta* fauna from Dabusu national key fossil locality, Jilin Province. *Geol. Bull. China* 35, 872–878. doi: 10.3969/j.issn.1671-2552.2016.06.004

Chen, X., Yang, M., and Zhao, H. (2023). Early Pleistocene mammal fossils from Niujuangou locality, Nihewan Basin, Hebei Province. *Quat. Sci.* 43, 763–776. doi: 10.11928/j.issn.1001-7410.2023.03.07

Chen, X., Zhao, H., Zhang, B., and Tong, H. (2017). Report on the excavation of the early Pleistocene Shigou site B in Nihewan Basin, northern China. *Quat. Sci.* 37, 895–907. doi: 10.11928/j.issn.1001-7410.2017.04.24

Ciner, B., Wang, Y., Deng, T., Flynn, L., Hou, S., and Wu, W. (2015). Stable carbon and oxygen isotopic evidence for Late Cenozoic environmental change in Northern China. *Palaeogeogr. Palaeoclimatol. Palaeoecol.* 440, 750–762. doi: 10.1016/j.palaeo.2015.10.009

Da, J., Zhang, Y. G., Wang, H., Balsam, W., and Ji, J. (2015). An Early Pleistocene atmospheric CO_2 record based on pedogenic carbonate from the Chinese loess deposits. *Earth Planet. Sci. Lett.* 426, 69–75. doi: 10.1016/j.epsl.2015.05.053

Dansgaard, W. (1964). Stable isotopes in precipitation. *Tellus* 16, 436–468. doi: 10.1111/tus.1964.16.issue-4

Deng, C., Xie, F., Liu, C., Ao, H., Pan, Y., and Zhu, R. (2007). Magnetochronology of the Feiliang Paleolithic site in the Nihewan Basin and implications for early human adaptability to high northern latitudes in East Asia. *Geophys. Res. Lett.* 34, L14301. doi: 10.1029/2007GL030335

Deng, T. (2002). The earliest known wooly rhino discovered in the Linxia Basin, Gansu Province, China. *Geol. Bull. China* 21, 604–608. doi: 10.3969/j.issn.1671-2552.2002.10.002

Deng, T. (2006). Neogene rhinoceroses of the Linxia basin (Gansu, China). *Cour.-Forschungsinstitut Senckenberg* 256, 43–56.

Deng, T. (2008). Comparison between woolly rhino forelimbs from Longdan, Northwestern China and Tologoi, Transbaikalian region. *Quat. Int.* 179, 196–207. doi: 10.1016/j.quaint.2007.09.008

Deng, T., Li, Q., Tseng, Z. J.J., Takeuchi, G. T., Wang, Y., Xie, G. P., et al. (2012). Locomotive implication of a Pliocene three-toed horse skeleton from Tibet and its paleo-altimetry significance. *Proc. Natl. Acad. Sci.* 109, 7374–7378. doi: 10.1073/pnas.1201052109

Deng, T., Lu, X., Sun, D., and Li, S. (2023). Rhinocerotoid fossils of the Linxia Basin in northwestern China as late Cenozoic biostratigraphic markers. *Palaeogeogr. Palaeoclimatol. Palaeoecol.* 614, 111427. doi: 10.1016/j.palaeo.2023.111427

Deng, T., Qiu, Z. X., Wang, B. Y., Wang, X. M., and Hou, S. K. (2013). "Late Cenozoic biostratigraphy of the Linxia Basin, northwestern China," in *Fossil Mammals of Asia: Neogene Biostratigraphy and Chronology*. Eds. Wang, X. M., Flynn, L. J., and Fortelius, M. (Columbia University Press, New York), 243–273.

Deng, T., Wang, X., Fortelius, M., Li, Q., Wang, Y., Tseng, Z. J., et al. (2011). Out of Tibet: Pliocene woolly rhino suggests high-plateau origin of Ice Age megaherbivores. *Science* 333, 1285–1288. doi: 10.1126/science.1206594

Dettman, D. L., Fang, X., Garzione, C. N., and Li, J. (2003). Uplift-driven climate change at 12 Ma: a long $\delta^{18}O$ record from the NE margin of the Tibetan plateau. *Earth Planet. Sci. Lett.* 214, 267–277. doi: 10.1016/S0012-821X(03)00383-2

Dong, W., Bai, W.-P., and Zhang, L.-M. (2021). The first description of Rhinocerotidae (Perissodactyla, Mammalia) from Xinyaozi Ravine in Shanxi, North China. *Vertebr. Palasiat.* 59, 273–294. doi: 10.19615/j.cnki.2096-9899.210715

Dong, W., Hou, Y., Yang, Z., Zhang, L., Zhang, S., and Liu, Y. (2014). Late Pleistocene mammalian fauna from Wulanmulan Paleolithic Site, Nei Mongol, China. *Quat. Int.* 347, 139–147. doi: 10.1016/j.quaint.2014.05.051

Dutton, A., Wilkinson, B. H., Welker, J. M., Bowen, G. J., and Lohmann, K. C. (2005). Spatial distribution and seasonal variation in $^{18}O/^{16}O$ of modern precipitation and river water across the conterminous USA. *Hydrol. Process.* 19, 4121–4146. doi: 10.1002/hyp.5876

Farjand, A., Zhang, Z., Gibbard, P. L., and Bi, S. (2023a). First results of the biostratigraphy and geochronology of the classic Nihewan Fauna, China. *Front. Earth Sci.* 11, 1276816. doi: 10.3389/feart.2023.1276816

Farjand, A., Zhang, Z., Kaakinen, A., Bi, S., Gibbard, P. L., and Lihua, W. (2023b). Rediscovery and stratigraphic calibration of the classic Nihewan Fauna, Hebei Province, China. *Quat. Int.* 646, 1–10. doi: 10.1016/j.quaint.2022.12.001

Farquhar, G. D., Ehleringer, J. R., and Hubick, K. T. (1989). Carbon isotope discrimination and photosynthesis. *Annu. Rev. Plant Biol.* 40, 503–537. doi: 10.1146/annurev.pp.40.060189.002443

Fortelius, M. (1983). The morphology and paleobiological significance of the horns of *Coelodonta antiquitatis* (Mammalia: Rhinocerotidae). *J. Vertebr. Paleontol.* 3, 125–135. doi: 10.1080/02724634.1983.10011964

Green, D. R., Smith, T. M., Green, G. M., Bidlack, F. B., Tafforeau, P., and Colman, A. S. (2018). Quantitative reconstruction of seasonality from stable isotopes in teeth. *Geochim. Cosmochim. Acta* 235, 483–504. doi: 10.1016/j.gca.2018.06.013

Hammer, Ø., Harper, D. A. T., and Ryan, P. D. (2001). PAST: paleontological statistics software package for education and data analysis. *Electron* 4, 9.

Higgins, P., and MacFadden, B. J. (2004). "Amount Effect" recorded in oxygen isotopes of Late Glacial horse (*Equus*) and bison (*Bison*) teeth from the Sonoran and Chihuahuan deserts, southwestern United States. *Palaeogeogr. Palaeoclimatol. Palaeoecol.* 206, 337–353. doi: 10.1016/j.palaeo.2004.01.011

Hillson, S. (2005). *Teeth* (Cambridge: Cambridge university press). doi: 10.1017/CBO9780511614477

Hodgkins, J., Marean, C. W., Venter, J. A., Richardson, L., Roberts, P., Zech, J., et al. (2020). An isotopic test of the seasonal migration hypothesis for large grazing ungulates inhabiting the Palaeo-Agulhas Plain. *Quat. Sci. Rev.* 235, 106221. doi: 10.1016/j.quascirev.2020.106221

Hough, B. G., Garzione, C. N., Wang, Z., Lease, R. O., Burbank, D. W., and Yuan, D. (2011). Stable isotope evidence for topographic growth and basin segmentation: Implications for the evolution of the NE Tibetan Plateau. *Geol. Soc Am. Bull.* 123, 168–185. doi: 10.1130/B30090.1

Jin, C., Wang, Y., Liu, J., Ge, J., Zhao, B., Liu, J., et al. (2021). Late Cenozoic mammalian faunal evolution from Jinyuan Cave at Luotuo Hill from Dalian, Northeast China. *Quat. Int.* 577, 15–28. doi: 10.1016/j.quaint.2021.01.011

Kahlke, R.-D. (1999). *The history of the origin, evolution and dispersal of the Late Pleistocene Mammuthus-Coelodonta Faunal Complex in Eurasia (large mammals)* (Rapid City: Fenske Companies).

Kahlke, R.-D. (2014). The origin of Eurasian Mammoth Faunas (*Mammuthus–Coelodonta* Faunal Complex). *Quat. Sci. Rev.* 96, 32–49. doi: 10.1016/j.quascirev.2013.01.012

Kahlke, R.-D., and Lacombat, F. (2008). The earliest immigration of woolly rhinoceros (*Coelodonta tologoijensis*, Rhinocerotidae, Mammalia) into Europe and its adaptive evolution in Palaearctic cold stage mammal faunas. *Quat. Sci. Rev.* 27, 1951–1961. doi: 10.1016/j.quascirev.2008.07.013

Kassambara, A. (2020). *ggpubr: "ggplot2" Based Publication Ready Plots* (R package version 0.4.0).

Koch, P. L., Fisher, D. C., and Dettman, D. (1989). Oxygen isotope variation in the tusks of extinct proboscideans: A measure of season of death and seasonality. *Geology* 17, 515–519. doi: 10.1130/0091-7613(1989)017<0515:OIVITT>2.3.CO;2

Kohn, M. J. (2010). Carbon isotope compositions of terrestrial C_3 plants as indicators of (paleo) ecology and (paleo) climate. *Proc. Natl. Acad. Sci.* 107, 19691–19695. doi: 10.1073/pnas.1004933107

Kohn, M. J., and Cerling, T. E. (2002). Stable isotope compositions of biological apatite. *Rev. Mineral. Geochem.* 48, 455–488. doi: 10.2138/rmg.2002.48.12

Kohn, M. J., Schoeninger, M. J., and Valley, J. W. (1998). Variability in oxygen isotope compositions of herbivore teeth: reflections of seasonality or developmental physiology? *Chem. Geol.* 152, 97–112. doi: 10.1016/S0009-2541(98)00099-0

Körner, C. h., Farquhar, G. D., and Wong, S. C. (1991). Carbon isotope discrimination by plants follows latitudinal and altitudinal trends. *Oecologia* 88, 30–40. doi: 10.1007/BF00328400

Krajcarz, M., Pacher, M., Krajcarz, M. T., Laughlan, L., Rabeder, G., Sabol, M., et al. (2016). Isotopic variability of cave bears ($\delta^{15}N$, $\delta^{13}C$) across Europe during MIS 3. *Quat. Sci. Rev.* 131, 51–72. doi: 10.1016/j.quascirev.2015.10.028

Li, Y., Deng, T., Hua, H., Zhang, Y., and Wang, J. (2020). Isotopic record of palaeodiet of a 7.4 Ma Hipparionine fauna from the central Loess Plateau, northern China: Palaeo-ecological and palaeo-climatic implications. *Chem. Geol.* 532, 119353. doi: 10.1016/j.chemgeo.2019.119353

Li, Z., and Dong, W. (2007). Mammalian fauna from the Lingjing paleolithic site in Xuchang, Henan Province. *Acta Anthropol. Sin.* 26, 345–360. doi: 10.3969/j.issn.1000-3193.2007.04.008

Li, F., Kuhn, S. L., Chen, F., Wang, Y., Southon, J., Peng, F., et al. (2018). The easternmost middle paleolithic (Mousterian) from Jinsitai Cave, north China. *J. Hum. Evol.* 114, 76–84. doi: 10.1016/j.jhevol.2017.10.004

Liu, P., Deng, C., li, S., Cai, S., Cheng, H., Yuan, B., et al. (2012). Magnetostratigraphic dating of the Xiashagou Fauna and implication for sequencing the mammalian faunas in the Nihewan Basin, North China. *Palaeogeogr. Palaeoclimatol. Palaeoecol.* 315-316, 75–85. doi: 10.1016/j.palaeo.2011.11.011

Ma, J., Sun, B., Bocherens, H., and Deng, T. (2023). Dietary niche reconstruction of Pliocene and Pleistocene Equidae from the Linxia Basin of northwestern China based on stable isotope analysis. *Palaeogeogr. Palaeoclimatol. Palaeoecol.* 614, 111416. doi: 10.1016/j.palaeo.2023.111416

Ma, J., Wang, Y., Baryshnikov, G. F., Drucker, D. G., McGrath, K., Zhang, H., et al. (2021). The *Mammuthus-Coelodonta* Faunal Complex at its southeastern limit: A biogeochemical paleoecology investigation in Northeast Asia. *Quat. Int.* 591, 93–106. doi: 10.1016/j.quaint.2020.12.024

Ma, J., Zhang, F., Wang, Y., and Hu, Y. (2017). Tracking the foraging behavior of *Mammuthus primigenius* from the Late Pleistocene of northeast China, using stable isotope analysis. *Quat. Sci.* 37, 885–894. doi: 10.11928/j.issn.1001-7410.2017.04.23

Männel, T. T., Auerswald, K., and Schnyder, H. (2007). Altitudinal gradients of grassland carbon and nitrogen isotope composition are recorded in the hair of grazers. *Glob. Ecol. Biogeogr.* 16, 583–592. doi: 10.1111/j.1466-8238.2007.00322.x

Negash, E. W., and Barr, W. A. (2023). Relative abundance of grazing and browsing herbivores is not a direct reflection of vegetation structure: Implications for hominin paleoenvironmental reconstruction. *J. Hum. Evol.* 177, 103328. doi: 10.1016/j.jhevol.2023.103328

O'Leary, M. H. (1981). Carbon isotope fractionation in plants. *Phytochemistry* 20, 553–567. doi: 10.1016/0031-9422(81)85134-5

Passey, B. H., Cerling, T. E., and Levin, N. E. (2007). Temperature dependence of oxygen isotope acid fractionation for modern and fossil tooth enamels. *Rapid Commun. Mass Spectrom.* 21, 2853–2859. doi: 10.1002/rcm.3149

Pederzani, S., and Britton, K. (2019). Oxygen isotopes in bioarchaeology: Principles and applications, challenges and opportunities. *Earth-Sci. Rev.* 188, 77–107. doi: 10.1016/j.earscirev.2018.11.005

Pei, S., Deng, C., de la Torre, I., Jia, Z., Ma, D., Li, X., et al. (2019). Magnetostratigraphic and archaeological records at the Early Pleistocene site complex of Madigou (Nihewan Basin): implications for human adaptations in North

China. *Palaeogeogr. Palaeoclimatol. Palaeoecol.* 530, 176–189. doi: 10.1016/j.palaeo.2019.05.014

Peuke, A. D., Gessler, A., and Rennenberg, H. (2006). The effect of drought on C and N stable isotopes in different fractions of leaves, stems and roots of sensitive and tolerant beech ecotypes. *Plant Cell Environ.* 29, 823–835. doi: 10.1111/j.1365-3040.2005.01452.x

Pushkina, D., Bocherens, H., and Ziegler, R. (2014). Unexpected palaeoecological features of the Middle and Late Pleistocene large herbivores in southwestern Germany revealed by stable isotopic abundances in tooth enamel. *Quat. Int.* 339–340, 164–178. doi: 10.1016/j.quaint.2013.12.033

Pushkina, D., Juha, S., Reinhard, Z., and Bocherens, H. (2020). Stable isotopic and mesowear reconstructions of paleodiet and habitat of the Middle and Late Pleistocene mammals in south-western Germany. *Quat. Sci. Rev.* 227, 106026. doi: 10.1016/j.quascirev.2019.106026

Qiu, Z. (2000). Nihewan fauna and Q/N boundary in China. *Quat. Sci.* 20, 142–154.

Qiu, Z., Deng, T., and Wang, B. (2004). *Early Pleistocene mammalian fauna from Longdan, Dongxiang, Gansu, China* (Beijing: Science Press).

Qiu, Z., Wang, B., Deng, T., Ni, X., and Wang, X. (2002). Notes on the mammal fauna from the bottom of loess deposits at Longdan, Dongxiang County, Gansu Province. *Quat. Sci.* 22, 33–38. doi: 10.3321/j.issn:1001-7410.2002.01.006

Quade, J., Cerling, T. E., Andrews, P., and Alpagut, B. (1995). Paleodietary reconstruction of Miocene faunas from Paşalar, Turkey using stable carbon and oxygen isotopes of fossil tooth enamel. *J. Hum. Evol.* 28, 373–384. doi: 10.1006/jhev.1995.1029

Ransom, J. I., and Kaczensky, P. (2016). *Wild equids: Ecology, management, and conservation* (Baltimore: Johns Hopkins University Press). doi: 10.1353/book.47460

Rey-Iglesia, A., Lister, A. M., Stuart, A. J., Bocherens, H., Szpak, P., Willerslev, E., et al. (2021). Late Pleistocene paleoecology and phylogeography of woolly rhinoceros. *Quat. Sci. Rev.* 263, 106993. doi: 10.1016/j.quascirev.2021.106993

Rivals, F., and Álvarez-Lao, D. J. (2018). Ungulate dietary traits and plasticity in zones of ecological transition inferred from late Pleistocene assemblages at Jou Puerta and Rexidora in the Cantabrian Region of northern Spain. *Palaeogeogr. Palaeoclimatol. Palaeoecol.* 499, 123–130. doi: 10.1016/j.palaeo.2018.03.024

Rivals, F., and Lister, A. M. (2016). Dietary flexibility and niche partitioning of large herbivores through the Pleistocene of Britain. *Quat. Sci. Rev.* 146, 116–133. doi: 10.1016/j.quascirev.2016.06.007

Rivals, F., Mihlbachler, M. C., Solounias, N., Mol, D., Semprebon, G. M., de Vos, J., et al. (2010). Palaeoecology of the Mammoth Steppe fauna from the late Pleistocene of the North Sea and Alaska: Separating species preferences from geographic influence in paleoecological dental wear analysis. *Palaeogeogr. Palaeoclimatol. Palaeoecol.* 286, 42–54. doi: 10.1016/j.palaeo.2009.12.002

Roberts, P., Stewart, M., Alagaili, A. N., Breeze, P., Candy, I., Drake, N., et al. (2018). Fossil herbivore stable isotopes reveal middle Pleistocene hominin palaeoenvironment in 'Green Arabia'. *Nat. Ecol. Evol.* 2, 1871–1878. doi: 10.1038/s41559-018-0698-9

Rozanski, K., Araguás-Araguás, L., and Gonfiantini, R. (1993). Isotopic patterns in modern global precipitation. *Clim. Change Cont. Isot. Rec.*. Eds. P. K. Swart, K. C. Lohmann, J. A. McKenzie and S. Savin (American Geophysical Union, Washington), 1–36. doi: 10.1029/gm078p0001

RStudio Team (2016). *RStudio: integrated development for R (Version 1.1. 423)* (Boston: RStudio Inc.).

Schreve, D. C. (2001). Differentiation of the British late Middle Pleistocene interglacials: the evidence from mammalian biostratigraphy. *Quat. Sci. Rev.* 20, 1693–1705. doi: 10.1016/S0277-3791(01)00033-6

Schreve, D. (2019). All is flux: the predictive power of fluctuating Quaternary mammalian faunal-climate scenarios. *Philos. Trans. R. Soc B Biol. Sci.* 374, 20190213. doi: 10.1098/rstb.2019.0213

Schwartz-Narbonne, R., Longstaffe, F. J., Kardynal, K. J., Druckenmiller, P., Hobson, K. A., Jass, C. N., et al. (2019). Reframing the mammoth steppe: Insights from analysis of isotopic niches. *Quat. Sci. Rev.* 215, 1–21. doi: 10.1016/j.quascirev.2019.04.025

Sharp, Z. D., and Cerling, T. E. (1998). Fossil isotope records of seasonal climate and ecology: Straight from the horse's mouth. *Geology* 26, 219–222. doi: 10.1130/0091-7613 (1998)026<0219:FIROSC>2.3.CO;2

Smith, B. N., and Epsten, S. (1971). Two categories of $^{13}C/^{12}C$ ratios for higher plants. *Plant Physiol.* 47, 380–384. doi: 10.1104/pp.47.3.380

Smith, T. M., Martin, L. B., and Leakey, M. G. (2003). Enamel thickness, microstructure and development in *Afropithecus turkanensis*. *J. Hum. Evol.* 44, 283–306. doi: 10.1016/S0047-2484(03)00006-X

Sokolowski, K. G., Codding, B. F., Du, A., and Faith, J. T. (2023). Do grazers equal grasslands? Strengthening paleoenvironmental inferences through analysis of present-day African mammals. *Palaeogeogr. Palaeoclimatol. Palaeoecol.* 629, 111786. doi: 10.1016/j.palaeo.2023.111786

Sponheimer, M., and Lee-Thorp, J. A. (1999). Oxygen isotopes in enamel carbonate and their ecological significance. *J. Archaeol. Sci.* 26, 723–728. doi: 10.1006/jasc.1998.0388

Stefaniak, K., Kovalchuk, O., Ratajczak-Skrzatek, U., Kropczyk, A., Mackiewicz, P., Kłys, G., et al. (2023). Chronology and distribution of Central and Eastern European Pleistocene rhinoceros (Perissodactyla, Rhinocerotidae) – A review. *Quat. Int.* 674–675, 87–108. doi: 10.1016/j.quaint.2023.02.004

Stefaniak, K., Stachowicz-Rybka, R., Borówka, R. K., Hrynowiecka, A., Sobczyk, A., Moskal-del Hoyo, M., et al. (2021). Browsers, grazers or mix-feeders? Study of the diet of extinct Pleistocene Eurasian forest rhinoceros *Stephanorhinus kirchbergensis* (Jäger 1839) and woolly rhinoceros *Coelodonta antiquitatis* (Blumenbach 1799). *Quat. Int.* 605–606, 192–212. doi: 10.1016/j.quaint.2020.08.039

Stuart, A. J., and Lister, A. M. (2012). Extinction chronology of the woolly rhinoceros *Coelodonta antiquitatis* in the context of late Quaternary megafaunal extinctions in northern Eurasia. *Quat. Sci. Rev.* 51, 1–17. doi: 10.1016/j.quascirev.2012.06.007

Suga, S. (1979). Comparative histology of progressive mineralization pattern of developing incisor enamel of rodents. *J. Dent. Res.* 58, 1025–1026. doi: 10.1177/00220345790580021401

Tang, Z., Liu, S., Lin, Z., and Liu, H. (2003). The late Pleistocene fauna from Dabusu of Qian'an in Jilin province of China. *Vertebr. Palasiat.* 41, 145–153. doi: 10.3969/j.issn.1000-3118.2003.02.005

Tejada-Lara, J. V., MacFadden, B. J., Bermudez, L., Rojas, G., Salas-Gismondi, R., and Flynn, J. J. (2018). Body mass predicts isotope enrichment in herbivorous mammals. *Proc. R. Soc B Biol. Sci.* 285, 20181020. doi: 10.1098/rspb.2018.1020

Tiunov, A. V., and Kirillova, I. V. (2010). Stable isotope ($^{13}C/^{12}C$ and $^{15}N/^{14}N$) composition of the woolly rhinoceros *Coelodonta antiquitatis* horn suggests seasonal changes in the diet. *Rapid Commun. Mass Spectrom.* 24, 3146–3150. doi: 10.1002/rcm.4755

Tong, H. (2004). Paleoenvironmental significance of *Coelodonta* in different fossil assembledges. *Acta Anthr. Sin.* 23 (suppl.), 306–314.

Tong, H., Li, H., and Xie, J. (2008). Revisions of some taxa of the Salawusu fauna from Sjara-Osso-Gol area, Nei Mongol, China. *Quat. Sci.* 28, 1106–1113. doi: 10.3321/j.issn:1001-7410.2008.06.016

Tong, H., and Wang, X. (2014). Juvenile skulls and other postcranial bones of *Coelodonta nihowanensis* from Shanshenmiaozui, Nihewan Basin, China. *J. Vertebr. Paleontol.* 34, 710–724. doi: 10.1080/02724634.2013.814661

Tong, H., Zhang, B., Chen, X., Wang, X., and Sun, J. (2021). Chronological significance of the mammalian fauna from the Early Pleistocene Shanshenmiaozui site in Nihewan Basin, northern China. *Acta Anthr. Sin.* 40, 469–489. doi: 10.16359/j.1000-3193/AAS.2021.0026

Troughton, J. H., and Card, K. A. (1975). Temperature effects on the carbon-isotope ratio of C_3, C_4 and crassulacean-acid-metabolism (CAM) plants. *Planta* 123, 185–190. doi: 10.1007/BF00383867

Uzunidis, A., Antoine, P.-O., and Brugal, J.-P. (2022). A Middle Pleistocene *Coelodonta antiquitatis praecursor* (Mammalia, Perissodactyla) from Les Rameaux, SW France, and a revised phylogeny of *Coelodonta*. *Quat. Sci. Rev.* 288, 107594. doi: 10.1016/j.quascirev.2022.107594

van der Merwe, N. J., and Medina, E. (1991). The canopy effect, carbon isotope ratios and foodwebs in Amazonia. *J. Archaeol. Sci.* 18, 249–259. doi: 10.1016/0305-4403(91)90064-V

van Geel, B., Langeveld, B. W., Mol, D., van der Knaap, P. W. O., and van Leeuwen, J. F. N. (2019). Pollen and spores from molar folds reflect food choice of late Pleistocene and Early Holocene herbivores in The Netherlands and the adjacent North Sea area. *Quat. Sci. Rev.* 225, 106030. doi: 10.1016/j.quascirev.2019.106030

Wang, B. (2005). Beaver (Rodentia, mammalial) fossils from Longdan, Gansu, China. *Vertebr. Palasiat.* 43, 237–242. doi: 10.3969/j.issn.1000-3118.2005.03.008

Wang, Y., and Deng, T. (2005). A 25 m.y. isotopic record of paleodiet and environmental change from fossil mammals and paleosols from the NE margin of the Tibetan Plateau. *Earth Planet. Sci. Lett.* 236, 322–338. doi: 10.1016/j.epsl.2005.05.006

Wang, H., Deng, C., Zhu, R., Wei, Q., Hou, Y., and Boëda, E. (2005). Magnetostratigraphic dating of the Donggutuo and Maliang Paleolithic sites in the Nihewan Basin, North China. *Quat. Res.* 64, 1–11. doi: 10.1016/j.yqres.2005.04.001

Wang, Y., Kromhout, E., Zhang, C., Xu, Y., Parker, W., Deng, T., et al. (2008a). Stable isotopic variations in modern herbivore tooth enamel, plants and water on the Tibetan Plateau: Implications for paleoclimate and paleoelevation reconstructions. *Palaeogeogr. Palaeoclimatol. Palaeoecol.* 260, 359–374. doi: 10.1016/j.palaeo.2007.11.012

Wang, H., Li, Z., Tong, H., and van Kolfschoten, T. (2021). Hominin paleoenvironment in East Asia: The Middle Paleolithic Xuchang-Lingjing (China) mammalian evidence. *Quat. Int.* 633, 118–133. doi: 10.1016/j.quaint.2021.11.024

Wang, X., Li, Q., Xie, G., Saylor, J. E., Tseng, Z. J., Takeuchi, G. T., et al. (2013). Mio-Pleistocene Zanda Basin biostratigraphy and geochronology, pre-Ice Age fauna, and mammalian evolution in western Himalaya. *Palaeogeogr. Palaeoclimatol. Palaeoecol.* 374, 81–95. doi: 10.1016/j.palaeo.2013.01.007

Wang, Y., Wang, X., Xu, Y., Zhang, C., Li, Q., Tseng, Z. J., et al. (2008b). Stable isotopes in fossil mammals, fish and shells from Kunlun Pass Basin, Tibetan Plateau: Paleo-climatic and paleo-elevation implications. *Earth Planet. Sci. Lett.* 270, 73–85. doi: 10.1016/j.epsl.2008.03.006

Wang, Y., Xu, Y., Khawaja, S., Passey, B. H., Zhang, C., Wang, X., et al. (2013). Diet and environment of a mid-Pliocene fauna from southwestern Himalaya: Paleo-elevation implications. *Earth Planet. Sci. Lett.* 376, 43–53. doi: 10.1016/j.epsl.2013.06.014

Wickham, H. (2011). ggplot2: Elegant Graphics for Data Analysis. *Wiley Interdisc. Rev. Comput. Stat.* 3, 180–185. doi: 10.1002/wics.147

Xu, Z., Pei, S., Hu, Y., de la Torre, I., and Ma, D. (2021). Stable isotope analysis of mammalian enamel from the Early Pleistocene site of Madigou, Nihewan Basin: Implications for reconstructing hominin paleoenvironmental adaptations in North China. *Front. Earth Sci.* 9, 789781. doi: 10.3389/feart.2021.789781

Xu, Z., Pei, S., Hu, Y., de la Torre, I., Ma, D., Ye, Z., et al. (2023). Ecological shifts and hominin adaptations during the Mid-Pleistocene Climate Transition in Northeast Asia as evidenced by isotopic analysis (δ^{13}C, δ^{18}O) of mammalian enamel from Early Paleolithic sites in the Nihewan Basin, China. *Quat. Sci. Rev.* 308, 108072. doi: 10.1016/j.quascirev.2023.108072

Xue, X., Zhang, Y., and Yue, L. (2006). Paleoenvironments indicated by the fossil mammalian assemblages from red clay-loess sequence in the Chinese Loess Plateau since 8.0 Ma B.P. *Sci. China Ser. D* 49, 518–530. doi: 10.1007/s11430-006-0518-y

Yang, S., Ding, Z., Wang, X., Tang, Z., and Gu, Z. (2012). Negative δ^{18}O–δ^{13}C relationship of pedogenic carbonate from northern China indicates a strong response of C_3/C_4 biomass to the seasonality of Asian monsoon precipitation. *Palaeogeogr. Palaeoclimatol. Palaeoecol.* 317–318, 32–40. doi: 10.1016/j.palaeo.2011.12.007

Zan, J., Fang, X., Zhang, W., Yan, M., and Zhang, T. (2016). Palaeoenvironmental and chronological constraints on the Early Pleistocene mammal fauna from loess deposits in the Linxia Basin, NE Tibetan Plateau. *Quat. Sci. Rev.* 148, 234–242. doi: 10.1016/j.quascirev.2016.07.026

Zhang, C., Wang, Y., Li, Q., Wang, X., Deng, T., Tseng, Z. J., et al. (2012). Diets and environments of late Cenozoic mammals in the Qaidam Basin, Tibetan Plateau: Evidence from stable isotopes. *Earth Planet. Sci. Lett.* 333–334, 70–82. doi: 10.1016/j.epsl.2012.04.013

Zhou, X., Yang, J., Wang, S., Xiao, G., Zhao, K., Zheng, Y., et al. (2018). Vegetation change and evolutionary response of large mammal fauna during the Mid-Pleistocene Transition in temperate northern East Asia. *Palaeogeogr. Palaeoclimatol. Palaeoecol.* 505, 287–294. doi: 10.1016/j.palaeo.2018.06.007